ACS OMEGA

http://pubs.acs.org/journal/acsodf

Article

Rapid Detection of IgM Antibodies against the SARS-CoV-2 Virus via Colloidal Gold Nanoparticle-Based Lateral-Flow Assay

Chao Huang,[†] Tian Wen,[†] Feng-Juan Shi, Xiao-Yan Zeng, and Yong-Jun Jiao*

Cite This: *ACS Omega* 2020, 5, 12550−12556

Read Online

ACCESS | Metrics & More | Article Recommendations | Supporting Information

ABSTRACT: Last year, the novel coronavirus disease (COVID-19) emerged in Wuhan, and it has rapidly spread to many other countries and regions. COVID-19 exhibits a strong human-to-human transmission infectivity and could cause acute respiratory diseases. Asymptomatic carriers are able to infect other healthy persons, and this poses a challenge for public health; the World Health Organization (WHO) has already announced COVID-19 as a global pandemic. Nucleic acid testing, considered as the current primary method for diagnosing COVID-19, might lead to false negatives and is difficult to be applied for every suspected patient because of the existence of asymptomatic carriers. Meanwhile, detecting specific antibodies in blood, such as the IgM antibody, against the SARS-CoV-2 virus is another choice for COVID-19 diagnosis, as it is widely accepted that IgM is an important indicator in the acute infection period. In this study, a colloidal gold nanoparticle-based lateral-flow (AuNP-LF) assay was developed to achieve rapid diagnosis and on-site detection of the IgM antibody against the SARS-CoV-2 virus through the indirect immunochromatography method. For preparing AuNP-LF strips, the SARS-CoV-2 nucleoprotein (SARS-CoV-2 NP) was coated on an analytical membrane for sample capture, and antihuman IgM was conjugated with AuNPs to form the detecting reporter. Optimization of AuNP-LF assay was carried out by altering the pH value and the amount of antihuman IgM. The performance of AuNP-LF assay was evaluated by testing serum samples of COVID-19 patients and normal humans. The results were compared with the real-time polymerase chain reaction. The sensitivity and specificity of AuNP-LF assay were determined to be 100 and 93.3%, respectively, and an almost perfect agreement was exhibited by Kappa statistics (κ coefficient = 0.872). AuNP-LF assay showed outstanding selectivity in the detection of IgM against the SARS-CoV-2 virus with no interference from other viruses such as severe fever with thrombocytopenia syndrome virus (SFTSV) and dengue virus (DFV). AuNP-LF assay was able to achieve results within 15 min and needed only 10−20 μL serum for each test. As a whole, in the light of its advantages such as excellent specificity and stability, easy operation, low cost, and being less time-consuming, AuNP-LF assay is a feasible method for the diagnosis of COVID-19 in primary hospitals and laboratories, especially in emergency situations in which numerous samples need to be tested on time.

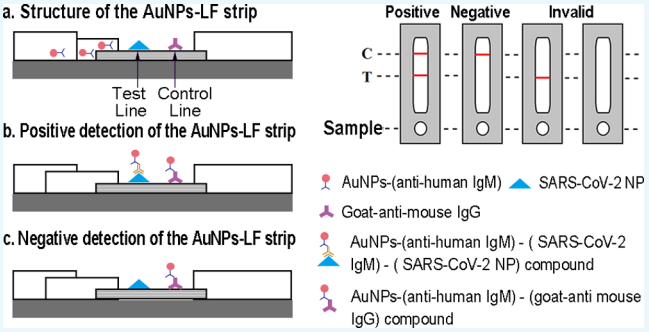

1. INTRODUCTION

In December 2019, the first pneumonia case of unknown etiological origins was reported in Wuhan city, China, and then, a series of similar cases emerged with the clinical symptoms of viral pneumonia.[1] Subsequently, high-throughput sequencing confirmed a novel coronavirus to be the causative pathogen, which is currently named 2019 novel coronavirus (SARS-CoV-2).[2] Coronaviruses, such as SARS-CoV in 2003[3−6] and MERS-CoV in 2012,[7] have infected humans several times and led to serious consequences in the past. Similarly, the infection of SARS-CoV-2 caused COVID-19. Because of the severe human-to-human transmission, the disease quickly spread all around China and almost the whole world and has become a globe public health emergency, as declared by the WHO.[8]

Although COVID-19 could cause severe lung damage and lead to patient's death, this disease also has many common clinical manifestations including fever, cough, myalgia, shortness of breath, and fatigue, and these symptoms are usually associated with other respiratory infections.[9] According to the guideline for COVID-19 diagnosis and treatment, real-time polymerase chain reaction (RT-PCR) is the predominant and standard method for laboratory diagnosis.[10] However, this method could not overcome some non-negligible drawbacks, including the long nucleic acid extraction procedure and nonsuitability for on-site detection. Also, false-negative results were unavoidable because of many factors, such as unstable reagents, low viral load in the sample, and improper sampling

Received: April 6, 2020
Accepted: May 5, 2020
Published: May 18, 2020

techniques.[11−14] More importantly, as a sophisticated detection method, RT-PCR relies more on operators' experiences and complex equipments, and the relative reagents need a cold chain support for both transportation and storage. All these factors will delay the detection efficiency. Hence, it is urgently needed to establish a rapid and easily performed method to facilitate the on-site diagnosis of COVID-19.

In addition to detecting the virus that COVID-19 patients carried, testing specific antibodies in serum is an alternative way to confirm SARS-CoV-2 infection, which was addressed by COVID-19 diagnosis and treatment guideline in China. For infectious diseases, the IgM amount in blood increases rapidly during the acute infection phase, whether the infected persons show clinical symptoms or not.[15] For example, IgM against the SARS virus could be detected in blood samples several days after the infection happened,[16,17] while asymptomatic Zika virus carriers still have IgM antibody in their blood.[18] For the above-mentioned reasons, developing a rapid detection method for IgM against SARS-CoV-2 will provide a valuable supplementary in the diagnosis of COVID-19.

Because of their several advantages, such as easy operation, low cost, real-time result feedback, and being independent of cold chain, rapid diagnosis strips are widely used in many point-of-care testing (POCT) applications.[19,20] Until now, a variety of signal reporters have been utilized, including colloidal gold nanoparticles,[21] magnetic nanoparticles,[22] upconverting nanoparticles,[23] quantum dots,[24] and fluorescein isothiocyanates.[25] POCT strips were mainly used in rapid detection of pregnancy and drug abuse during the early stage[26,27] and many kinds of infectious diseases recently.[28,29] The AuNP-LF assay is a rapidly developing technology, which utilizes colloidal gold nanoparticles, an easily synthesized and low-cost inorganic nanomaterials, as the reporter in immunoreactions.[30] In contrast with other reporting labels, AuNPs were considered to possess unique advantages of long-term stability, obvious eye-reading results, easy operation, and free of complex instruments. Furthermore, AuNPs exhibit excellent biocompatibility and little biological toxicity,[31−33] which is a great advantage in *in vitro* and *in vivo* diagnosis. Therefore, the POCT strip based on AuNP-LF assay is efficient for rapid on-site and low-cost detection because it gives easily observable positive or negative results. Until now, the AuNP-LF assay has been widely used to detect various analytes including infectious virus, proteins, drugs, and other pathogens.[34−37]

In this article, a rapid detection method for the IgM antibody against the SARS-CoV-2 virus, using the SARS-CoV-2 NP prepared by our group as the capture antigen, was designed and developed. This Au NP-LF assay combines the merits of the immune lateral-flow system and unique properties of AuNPs and is easily operated and cost-effective in large-scale detection. Especially, the whole test process lasts for less than 15 min to obtain results and requires only 10−20 μL serum. We discussed several factors in the preparation of colloidal gold immune conjugates and the manufacture of AuNP-LF strips. The sensitivity, specificity, and stability were evaluated by testing clinical positive and negative serum samples, with RT-PCR's test results as the control. Considering all the advantages of this newly developed AuNP-LF assay, it is possible for it to become an auxiliary diagnostic method for COVID-19 and has great potential in containing worldwide pandemic.

2. RESULTS AND DISCUSSION

2.1. Characterization of AuNPs. UV−vis absorption spectra of AuNPs are shown in Figure 1A, and the maximum

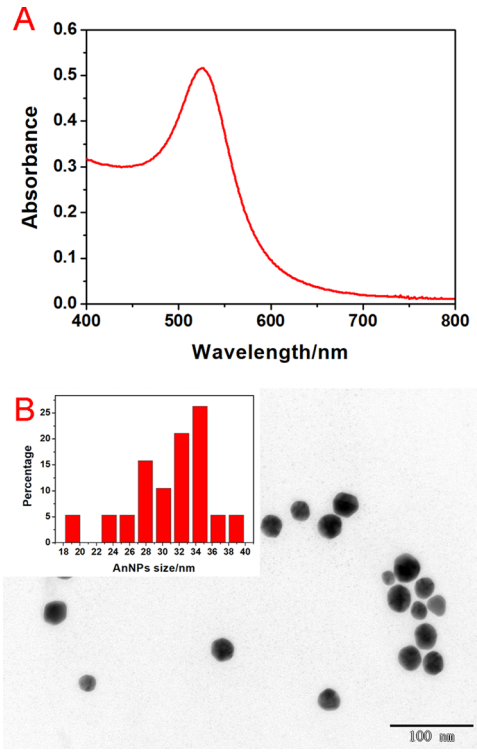

Figure 1. (A) TEM image of AuNPs. (B) UV−vis spectra of AuNPs.

ultraviolet absorption peak of AuNPs was located at 525 nm, which was coincident with the theoretical equation reported previously.[38] The obtained AuNPs have good distribution uniformity in the aqueous solution, which could be indicated from the narrow peak shape of UV−vis absorption spectra. As shown in Figure 1B, the transmission electron microscopy (TEM) image showed that AuNPs were about 30 nm in diameter. AuNPs of this size were suitable for conjugating proteins as the previous literature described.[39]

2.2. Optimization of AuNP−(Anti-Human IgM) Conjugates. As we know, when the reaction system's pH value is close or a little higher than the isoelectric point of the antibody, the electrostatic and physical adsorption between AuNPs and antibodies are most stable.[40,41] High concentration of salt will bring destructive effect into the reaction system. Figure S2A displayed that the reaction system's color under the optimal pH remained wine-red, while those under other pH changed to purple or even white. Hence, the optimal pH value was determined to be 8.0. Similarly, as shown in Figure S2B, 1.5 μg of anti-human IgM was sufficient to stabilize the conjugate. According to the previous literature,[42] 1.8 μg of anti-human IgM, slightly more than the above-mentioned antibody amount, was selected as the optimal level.

2.3. AuNP-LF Performance. The test performance of AuNP-LF mainly depended on several elements, such as protein coating concentration and nitrocellulose membrane block effects. Figure 2A showed the test results using different SARS-CoV-2 NP concentration (0.3, 0.6, 1.0, 1.2 mg/mL) coated on the test line (T line). When the COVID-19 positive serum sample was tested, the color intensity of the T line was

https://dx.doi.org/10.1021/acsomega.0c01554
ACS Omega 2020, 5, 12550−12556

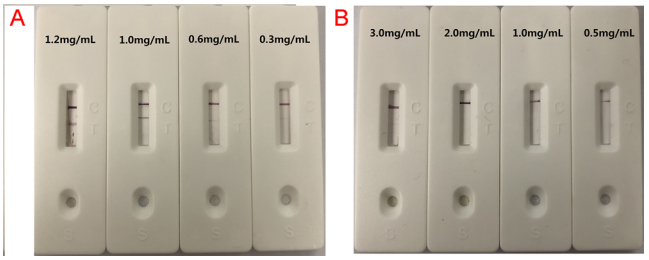

Figure 2. Performance of AuNP-LF based on different concentrations of (A) SARS-CoV-2 NP and (B) goat−anti-mouse IgG.

most significant with 1.2 mg/mL SARS-CoV-2 NP, but the flatness of the T line was not as good as 1.0 mg/mL SARS-CoV-2 NP. At lower concentrations, for example, 0.6 and 0.3 mg/mL, the red T line was difficult to be observed by naked eyes, so the optimal SARS-CoV-2 NP concentration was selected to be 1.0 mg/mL. Similarly, when normal persons' sera were tested, various concentrations of goat−anti-mouse IgG (0.5, 1.0, 2.0, 3.0 mg/mL) coated on the control line (C line) resulted in different visual effects (Figure 2B). Considering the intensity of the C line and antibody usage amount, 2.0 mg/mL goat−anti-mouse IgG was chosen for C line coating.

Another factor that had an impact on the performance of the AuNP-LF assay was the nitrocellulose membrane block effects. Different concentrations of bovine serum albumin (BSA) were blocked on the nitrocellulose membrane to reduce nonspecific adsorption. When normal human sera were tested, strips with 1.0 and 2.0 mg/mL BSA blocking did not show any T line signal, while the other two strips (0 and 0.5 mg/mL BSA blocking) showed false positives (Figure 3). For positive

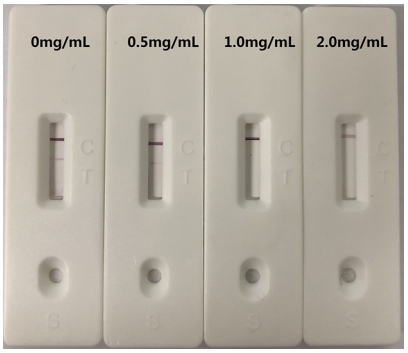

Figure 3. AuNP-LF performance based on nitrocellulose membrane block effects.

samples, all strips exhibited a visible red T line, while the strip with 2 mg/mL BSA blocking showed a pretty weak one. This indicated that excessive BSA would reduce AuNP-LF's sensitivity. From the above, we selected 1.0 mg/mL BSA to block the nitrocellulose membrane in order to eliminate nonspecific binding.

To study the performance of the AuNP-LF assay, the sensitivity of the test is also of significant importance. Nevertheless, when detecting antibodies using the immunochromatography method, the hook effect could not be neglected.[43] The hook effect results from the coinstantaneous reaction of an excess target protein with both immobilized and labeled antibodies or antigens. In this designed AuNP-LF assay, a larger amount of sera did not mean certain better sensitivity. A suitable proportion of serum and sample treating buffer took a significant role in improving the performance of the AuNP-LF assay. Different results were shown in Table S1. When 20 μL of the serum sample and 80 μL of treating buffer were mixed and tested, the result was much reliable than other conditions. For example, reducing serum to less than 10 μL might lead to incomplete absorption and result in misdetection. Conversely, excess serum had the chance to introduce a false positive phenomenon.

2.4. Specificity of the AuNP-LF Assay. Specificity is a key indicator in preventing the false-positive phenomenon from cross-reaction. One positive SARS-CoV-2 serum, two SFTSV sera, two DFV sera, and one normal human serum were tested using AuNP-LF strips. As shown in Figure 4, only

Figure 4. Specificity of AuNP-LF strips.

the SARS-CoV-2 strip displayed a legible red T line signal, while other strips showed no visible T lines. These results meant that there was not any cross-reactivity between SARS-CoV-2 and other listed viruses, which indicated the AuNP-LF's excellent specificity.

2.5. Stability and Reproducibility of the AuNP-LF Assay. The stability and reproducibility are of great practical value in POCT strips. Observed by naked eyes, the color depth at the T line revealed almost no differences at continuous detecting time points (1, 2, and 4 weeks) when SARS-CoV-2 samples were tested with SFTSV, DFV, and normal human serum samples as the control (Figure 5). Each sample was tested consecutive for ten times. This result demonstrated that our developed AuNP-LF assay possesses satisfactory stability.

2.6. Analysis Performance of the AuNP-LF Assay. The final purpose of the work was to establish a rapid and reliable method to detect the IgM antibody against the SARS-CoV-2 virus in COVID-19 patients' serum directly by naked eyes. In order to evaluate AuNP-LF's practicality, serum samples from five patients infected by SARS-CoV-2 (confirmed by RT-PCR) were collected and tested using our prepared strips, while normal humans' serum samples were assessed as the control. As shown in Figure S3 and Table 1, five RT-PCR-confirmed serum samples were all determined to be seropositive by AuNP-LF strips. Meanwhile, 13 out of 14 normal humans' sera were detected to be negative by our AuNP-LF assay, and only one sample was tested to be positive. Comprehensively analyzing the test results of the RT-PCR and AuNP-LF assay, our strips had a good consistency by the Kappa test (κ coefficient = 0.872). The sensitivity and specificity of AuNP-LF were 100 and 93.3%, respectively, and the Youden index was 0.933. All the analysis indicators demonstrate that our designed unique AuNP-LF assay is suitable for rapid and on-site surveillance of SARS-CoV-2 infection.

https://dx.doi.org/10.1021/acsomega.0c01554
ACS Omega 2020, 5, 12550−12556

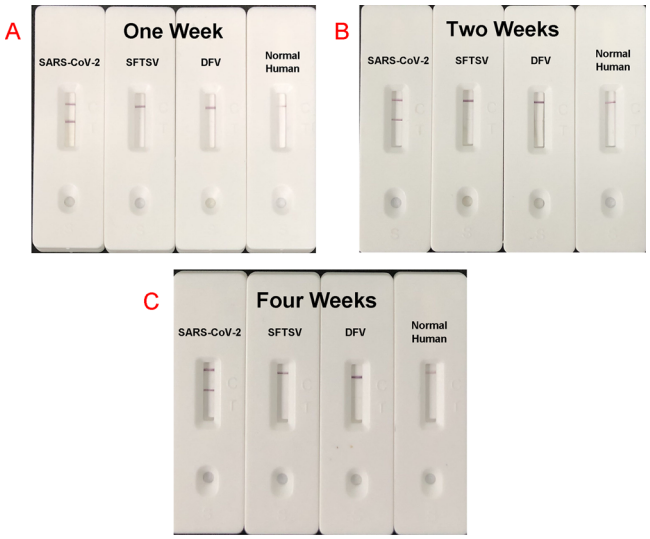

Figure 5. Stability of AuNP-LF strips.

Table 1. Statistical Comparisons between the AuNP-LF Assay and RT-PCR of COVID-19 Patients' and Normal Human's Serum[a]

		PCR method		
		+	−	total
AuNPs-LF assay	+	5	1	6
	−	0	13	13
	total	5	14	19

[a]Note: (+) positive result, (−) negative result.

All the results described above indicated that our designed AuNP-LF assay should have great significance in detecting the IgM antibody against the SARS-CoV-2 virus. In comparison with other traditional methods, the AuNP-LF assay exhibits several advantages as follows. First, AuNPs, employed to generate a test signal in the immunological technique, were stable and hard to be deactivated. Second, the sample consumption for each test was only 10−20 μL, while the nucleic acid extraction process of the RT-PCR usually required more than 100 μL of the sample. In addition to less sample usage, the total test time could be controlled within 15 min, while other test methods usually needed several hours. Furthermore, our designed AuNP-LF assay is particularly easy to practise, and the operators only need a minimal training, which means that tests could be carried out in any place, including primary hospitals and remote regions, as these facilities are usually lack sophisticated detection equipment and professional technicians. Meanwhile, the materials involved in assembling AuNP-LF strips, including colloidal gold nanoparticles, have excellent biocompatibility and biosecurity. In addition, the AuNP-LF assay does not need any instrument, and all the reagents and materials used in preparing strips are at a very low cost. Moreover, the AuNP-LF assay could avoid collecting patients' respiratory tract specimen, so the healthcare workers' risk of getting infected could be significantly reduced.

3. CONCLUSIONS

To sum up, we have fabricated AuNP-LF strips for rapid and on-site detection of the IgM antibody against the SARS-CoV-2 virus. In order to make the diagnosis of COVID-19 more accurate and reasonable, molecular and serological investigation should be applied simultaneously,[44,45] such as the widely used RT-PCR test and our designed AuNP-LF assay. In our developed POCT strips, AuNPs' unique features, such as excellent stability and simple synthesis, and the specific binding force between the matched antigen and antibody, were appropriately combined. Compared with the primarily used RT-PCR method, the AuNP-LF assay exhibits several superiorities including quick test time, less sample consumption, simplicity of operation, dispensing with expensive instruments, independence of professional experience, and much lower cost of each test. Also, as a reliable immunological detection, this proposed AuNP-LF assay has favorable specificity and repeatability. We tested both positive and negative SARS-CoV-2 serum samples, the result of the AuNP-LF assay has a good consistency with that of RT-PCR. As research continues, the newly developed method should have great potential in large-scale and fast detection, especially for urgent conditions, and will surely become an important supplementary diagnosis method for COVID-19.

4. MATERIALS AND METHODS

4.1. Materials and Chemicals. Chloroauric acid hydrated ($HAuCl_4$) and sodium citrate were purchased from Sigma-Aldrich (StLouis, MO, USA). Nitrocellulose membranes, glass fibers, absorbent papers, plastic cartridges for strips, goat antimouse IgG, and antihuman IgM were purchased from Shanghai JieYi Biotechnology Co.Ltd. (Shanghai, China). The SARS-CoV-2 NP was prepared and purified by our own research group. Serum samples of COVID-19 patients and normal human were obtained from the Jiangsu Provincial Center for Disease Prevention and Control. Other reagents are analytical pure and purchased from Sinopharm Chemical Reagent Co., Ltd (Shanghai, China). Ultrapure water used during the experiment was produced using a Millipore Milli-Q water purification system (Billerica. MA, USA).

4.2. Synthesis and Characterization of AuNPs. AuNPs of size ≈ 30 nm were fabricated according to the classical method with proper modifications,[46] and the specific steps of the synthesis process are described in the Supporting Information. A JEM-2100 transmission electron microscope (JEOL Ltd.) was used to measure the diameter and morphology of AuNPs, and the UV−vis absorption spectra of AuNPs were obtained using a Shimadzu UV-2600 spectrophotometer (Tokyo, Japan). All the photos in this article were taken with a digital camera by the authors.

4.3. Cloning and Expression of the SARS-CoV-2 NP. The recombinant SARS-CoV-2 NP was expressed and purified using the method that our group developed in other protein's production.[47] The detailed process was presented in the Supporting Information. Sodium dodecyl sulfate−polyacrylamide gel electrophoresis (SDS−PAGE) was applied to analyze the purified protein, and the result is shown in Figure S1. All operations were performed following the manufacturer's instructions.

4.4. Collection of Serum Samples. SARS-CoV-2-positive and -negative serum samples were applied in this study. All the sera were collected in Jiangsu province, China. Moreover, SFTSV and DFV sera were also collected for specificity evaluation.

4.5. Conjugation of Antihuman IgM to AuNPs. Before preparing the AuNP−(anti-human IgM) conjugate, the reaction condition including the pH value and antibody

https://dx.doi.org/10.1021/acsomega.0c01554
ACS Omega 2020, 5, 12550−12556

concentration, should be optimized. First, each centrifuge tube was filled with 200 μL of AuNP solution. The reaction system was adjusted to series of pH (6.5, 7.0, 7.5, 8.0, 8.5, 9.0, 9.5, and 10.0). Then, the labeled antibody was added into the mixture followed by a 10 min incubation at room temperature. Subsequently, 45 μL of 10% NaCl was added into the reaction system, and the mixture was incubated for another 2 h. Finally, the mixture's color changing was observed. Analogously, the optimization of the labeled antibody was studied by adding different amounts of antihuman IgM (0, 0.75, 1.5, 3.0, 4.5, 6.0, and 7.5 μg) into the reaction system. Under the optimal pH value and antibody amount, antihuman IgM was conjugated to the surface of AuNPs to form AuNP−(anti-human IgM) bioconjugates. First, 1 mL of AuNP solution was adjusted to the optimal pH, and then, 9 μg of anti-human IgM was added into the mixture and stirred for 30 min. Next, 250 μL of 5% (w/v) BSA solution was added to the reaction system with another 30 min stirring for blocking. Afterward, the products were collected by a two-step centrifugation. First, the solution was centrifuged at 2000 rpm for 10 min, and the impurity of large and inhomogenous particles were discarded. Second, the remained supernatant was centrifuged again at 13,200 rpm for another 10 min, and the sediment was kept. Finally, 500 μL of resuspension buffer [containing 0.5% (w/v) BSA, 0.5% (v/v) Tween-20, 2% (w/v) sucrose and 50 mM Tris] was used to resuspend the sediment products, and the AuNP−(anti-human IgM) conjugates were obtained.

4.6. Development of AuNP-LF Strips. The AuNP-LF strip is composed of a sample pad (10 × 4 mm), a conjugate pad (8 × 4 mm), a nitrocellulose membrane (20 × 4 mm), and an absorbent pad (10 × 4 mm). All these components are attached to a PVC backing card. The schematic diagram of the test strip is presented in Scheme 1. AuNP−(anti-human IgM) conjugates were immobilized on the conjugate pad, and then, the pad was dried at 37 °C for 1 h. The SARS-CoV-2 NP and goat antimouse IgG were dispensed on the nitrocellulose membrane at the concentration of 1.0 mg/mL for the T line and 2.0 mg/mL for the C line with the two lines' interval at 4 mm, and then, the nitrocellulose membrane was blocked using 1% (w/v) BSA for 30 min and dried at 37 °C for 2 h. Finally, the prepared strip was assembled into a plastic shell and stored in a vacuum bag for future use. During the manufacture process, one piece of the nitrocellulose membrane could produce at least 75 strips, so each strip was very cost-effective.

Scheme 1. Description of Operation Principle of the AuNP-LF Strip

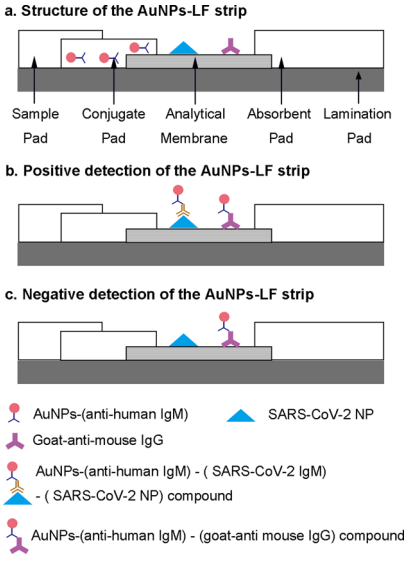

4.7. AuNPs-LF Assay Procedures. For detection, serum and sample treating buffer [30 mM PBS, pH 7.4, containing 1% (w/v) BSA, 0.1% (v/v) Triton X-100] were mixed at the desired ratio of 1:4, and then, 100 μL of the mixture was added onto the sample port of the AuNP-LF strip; then, the liquid transferred toward the absorbent pad under the hydrodynamic force and capillary power. During the test procedure, IgM in serum could be captured by the AuNP−(anti-human IgM) conjugate at the conjugate pad, and then, the AuNP−(anti-human IgM)−IgM compound flowed to the analytical membrane. The SARS-CoV-2 NP immobilized at the T line caught the target IgM against SARS-CoV-2 and form the AuNP−(anti-human IgM)−(SARS-CoV-2 IgM)−(SARS-CoV-2 NP) compound, while goat antimouse IgG immobilized at the C line directly caught AuNP−(anti-human IgM) and form the AuNP−(anti-human IgM)−(goat-anti mouse IgG) compound. The positive and negative results could be determined by the specific reddish-purple tracer of AuNPs. The red C line represents the strip's effectivity. If there was not a visible C line, whether a red T line appeared or not, the test result should be judged as invalid (Scheme 2). The detecting results could be easily judged by naked eyes within 15 min.

Scheme 2. Diagram of AuNP-LF Strips' Positive, Negative, and Invalid Results

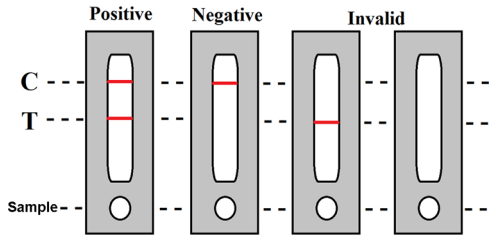

4.8. Specificity and Stability of the AuNP-LF Assay. Serum samples of several different diseases caused by other viruses were employed to study the specificity of the AuNP-LF assay, including SFTSV and DFV. The AuNP-LF strips used in this test belong to the same batch. Also, serum samples mentioned above were used to evaluate the stability of AuNP-LF strips. The strips were stored in cool, dry, airproof, and nonpollutuded conditions for different periods (1, 2, and 4 weeks). The test result was determined by the intensity of the T line which can easily be observed by the naked eyes.

4.9. Clinical Serum Samples Detection. Clinical specimens, including serum of clinically confirmed COVID-19 patients (positive) and normal humans (negative), were applied for the AuNP-LF assay, using RT-PCR as the contrast method. The consistency of the two methods was checked using the Kappa test.

■ ASSOCIATED CONTENT

Supporting Information

The Supporting Information is available free of charge at https://pubs.acs.org/doi/10.1021/acsomega.0c01554.

Synthesis of AuNPs, cloning and expression of SARS-CoV-2 NP, pretreatment of AuNPs-LF strips' conjugate

https://dx.doi.org/10.1021/acsomega.0c01554
ACS Omega 2020, 5, 12550−12556

pads, and SDS−PAGE result of SARS-CoV-2 NP, optimization of AuNPs−(anti-human IgM) bioconjugates, and photos of COVID-19 confirmed patients' and normal human's serum samples analysis by AuNPs-LF strips (PDF)

AUTHOR INFORMATION

Corresponding Author

Yong-Jun Jiao − *Key Laboratory of Enteric Pathogenic Microbiology, Ministry Health, Institute of Pathogenic Microbiology, Jiangsu Province Center for Disease Control and Prevention, Nanjing 210009, Jiangsu Province, P. R. China*; Email: yongjunjiao@163.com

Authors

Chao Huang − *Key Laboratory of Enteric Pathogenic Microbiology, Ministry Health, Institute of Pathogenic Microbiology, Jiangsu Province Center for Disease Control and Prevention, Nanjing 210009, Jiangsu Province, P. R. China*; orcid.org/0000-0002-4061-1573

Tian Wen − *Key Laboratory of Enteric Pathogenic Microbiology, Ministry Health, Institute of Pathogenic Microbiology, Jiangsu Province Center for Disease Control and Prevention, Nanjing 210009, Jiangsu Province, P. R. China*

Feng-Juan Shi − *Key Laboratory of Enteric Pathogenic Microbiology, Ministry Health, Institute of Pathogenic Microbiology, Jiangsu Province Center for Disease Control and Prevention, Nanjing 210009, Jiangsu Province, P. R. China*

Xiao-Yan Zeng − *Key Laboratory of Enteric Pathogenic Microbiology, Ministry Health, Institute of Pathogenic Microbiology, Jiangsu Province Center for Disease Control and Prevention, Nanjing 210009, Jiangsu Province, P. R. China*

Complete contact information is available at: https://pubs.acs.org/10.1021/acsomega.0c01554

Author Contributions

†C.H. and T.W. contributed equally to this work.

Notes

The authors declare no competing financial interest.

ACKNOWLEDGMENTS

This work was supported by the National Natural Science Foundation of China (81601732, 31700035, 31570926, and 81871666), the Natural Science Foundation of Jiangsu Province (BK20191489), the Key Research and Development Project of Jiangsu Province (BE2019761), and the Jiangsu provincial Medical Youth Talent (QNRC2016537 and JKRC2016018) and "Six One" Project (LGY2017084).

REFERENCES

(1) Lu, H.; Stratton, C. W.; Tang, Y. W. Outbreak of Pneumonia of Unknown Etiology in Wuhan China: the Mystery and the Miracle. *J. Med. Virol.* **2020**, *92*, 401−402.

(2) Zhu, N.; Zhang, D.; Wang, W.; Li, X.; Yang, B.; Song, J.; Zhao, X.; Huang, B.; Shi, W.; Lu, R.; Niu, P.; Zhan, F.; Ma, X.; Wang, D.; Xu, W.; Wu, G.; Gao, G. F.; Tan, W. A Novel Coronavirus from Patients with Pneumonia in China, 2019. *N. Engl. J. Med.* **2020**, *382*, 727−733.

(3) Zhong, N.; Zheng, B.; Li, Y.; Poon, L.; Xie, Z.; Chan, K.; Li, P.; Tan, S.; Chang, Q.; Xie, J.; Liu, X.; Xu, J.; Li, D.; Yuen, K.; Peiris, J.; Guan, Y. Epidemiology and cause of severe acute respiratory syndrome (SARS) in Guangdong, People's Republic of China, in February, 2003. *Lancet* **2003**, *362*, 1353−1358.

(4) Ksiazek, T. G.; Erdman, D.; Goldsmith, C. S.; Zaki, S. R.; Peret, T.; Emery, S.; Tong, S.; Urbani, C.; Comer, J. A.; Lim, W.; Rollin, P. E.; Dowell, S. F.; Ling, A.-E.; Humphrey, C. D.; Shieh, W.-J.; Guarner, J.; Paddock, C. D.; Rota, P.; Fields, B.; DeRisi, J.; Yang, J.-Y.; Cox, N.; Hughes, J. M.; LeDuc, J. W.; Bellini, W. J.; Anderson, L. J. A novel coronavirus associated with severe acute respiratory syndrome. *N. Engl. J. Med.* **2003**, *348*, 1953−1966.

(5) Drosten, C.; Günther, S.; Preiser, W.; van der Werf, S.; Brodt, H.-R.; Becker, S.; Rabenau, H.; Panning, M.; Kolesnikova, L.; Fouchier, R. A. M.; Berger, A.; Burguière, A.-M.; Cinatl, J.; Eickmann, M.; Escriou, N.; Grywna, K.; Kramme, S.; Manuguerra, J.-C.; Müller, S.; Rickerts, V.; Stürmer, M.; Vieth, S.; Klenk, H.-D.; Osterhaus, A. D. M. E.; Schmitz, H.; Doerr, H. W. Identification of a novel coronavirus in patients with severe acute respiratory syndrome. *N. Engl. J. Med.* **2003**, *348*, 1967−1976.

(6) Kuiken, T.; Fouchier, R. A.; Schutten, M.; Rimmelzwaan, G. F.; van Amerongen, G.; van Riel, D.; Laman, J. D.; de Jong, T.; van Doornum, G.; Lim, W.; Ling, A. E.; Chan, P. K.; Tam, J. S.; Zambon, M. C.; Gopal, R.; Drosten, C.; van der Werf, S.; Escriou, N.; Manuguerra, J.-C.; Stöhr, K.; Peiris, J. S. M.; Osterhaus, A. D. Newly discovered coronavirus as the primary cause of severe acute respiratory syndrome. *Lancet* **2003**, *362*, 263−270.

(7) Zaki, A. M.; van Boheemen, S.; Bestebroer, T. M.; Osterhaus, A. D. M. E.; Fouchier, R. A. M. Isolation of a Novel Coronavirus from a Man with Pneumonia in Saudi Arabia. *N. Engl. J. Med.* **2012**, *367*, 1814−1820.

(8) Huang, C.; Wang, Y.; Li, X.; Ren, L.; Zhao, J.; Hu, Y.; Zhang, L.; Fan, G.; Xu, J.; Gu, X.; Cheng, Z.; Yu, T.; Xia, J.; Wei, Y.; Wu, W.; Xie, X.; Yin, W.; Li, H.; Liu, M.; Xiao, Y.; Gao, H.; Guo, L.; Xie, J.; Wang, G.; Jiang, R.; Gao, Z.; Jin, Q.; Wang, J.; Cao, B. Clinical features of patients infected with 2019 novel coronavirus in Wuhan, China. *Lancet* **2020**, *395*, 497−506.

(9) Guan, W.-j.; Ni, Z.-y.; Hu, Y.; Liang, W.-h.; Ou, C.-q.; He, J.-x.; Liu, L.; Shan, H.; Lei, C.-l.; Hui, D.; Du, B.; Li, L.-j.; Zeng, G.; Yuen, K.-Y.; Chen, R.-c.; Tang, C.-l.; Wang, T.; Chen, P.-y.; Xiang, J.; Li, S.-y.; Wang, J.-l.; Liang, Z.-j.; Peng, Y.-x.; Wei, L.; Liu, Y.; Hu, Y.-h.; Peng, P.; Wang, J.-m.; Liu, J.-y..; Chen, Z.; Li, G.; Zheng, Z.-j.; Qiu, S.-q.; Luo, J.; Ye, C.-j.; Zhu, S.-y.; Zhong, N.-s. Clinical Characteristics of Coronavirus Disease2019 in China. *N. Engl. J. Med.* **2020**, *382*, 1708.

(10) Jin, Y.-H.; Cai, L.; Cheng, Z.-S.; Cheng, H.; Deng, T.; Fan, Y.-P.; Fang, C.; Huang, D.; Huang, L.-Q.; Huang, Q.; Han, Y.; Hu, B.; Hu, F.; Li, B.-H.; Li, Y.-R.; Liang, K.; Lin, L.-K.; Luo, L.-S.; Ma, J.; Ma, L.-L.; Peng, Z.-Y.; Pan, Y.-B.; Pan, Z.-Y.; Ren, X.-Q.; Sun, H.-M.; Wang, Y.; Wang, Y.-Y.; Weng, H.; Wei, C.-J.; Wu, D.-F.; Xia, J.; Xiong, Y.; Xu, H.-B.; Yao, X.-M.; Yuan, Y.-F.; Ye, T.-S.; Zhang, X.-C.; Zhang, Y.-W.; Zhang, Y.-G.; Zhang, H.-M.; Zhao, Y.; Zhao, M.-J.; Zi, H.; Zeng, X.-T.; Wang, Y.-Y.; Wang, X.-H. A rapid advice guideline for the diagnosis and treatment of 2019 novel coronavirus (COVID-19) infected pneumonia (standard version). *Mil. Med. Res.* **2020**, *7*, 4.

(11) Bacich, D.; Sobek, K.; Cummings, J.; Atwood, A.; O'Keefe, D. False negative results from using common PCR reagents. *BMC Res. Notes* **2011**, *4*, 457−463.

(12) Li, D.; Wang, D.; Dong, J.; Wang, N.; Huang, H.; Xu, H.; Xia, C. False-Negative Results of Real-Time Reverse-Transcriptase Polymerase Chain Reaction for Severe Acute Respiratory Syndrome Coronavirus 2: Role of Deep-Learning-Based CT Diagnosis and Insights from Two Cases. *Korean J. Radiol.* **2020**, *21*, 505−508.

(13) Ai, T.; Yang, Z.; Hou, H.; Zhan, C.; Chen, C.; Lv, W.; Tao, Q.; Sun, Z.; Xia, L. Correlation of Chest CT and RT-PCR Testing in Coronavirus Disease 2019 (COVID-19) in China: A Report of 1014 Cases. *Radiology* **2020**, 200642.

(14) Winichakoon, P.; Chaiwarith, R.; Liwsrisakun, C.; Salee, P.; Goonna, A.; Limsukon, A.; Kaewpoowat, Q. Negative Nasopharyngeal and Oropharyngeal Swab Does Not Rule Out COVID-19. *J. Clin. Microbiol.* **2020**, *58*, No. e00297.

(15) Boyle, M. J.; Chan, J. A.; Handayuni, I.; Reiling, L.; Feng, G.; Hilton, A.; Kurtovic, L.; Oyong, D.; Piera, K. A.; Barber, B. E.; William, T.; Eisen, D. P.; Minigo, G.; Langer, C.; Drew, D. R.; Rivera, F.; Amante, F. H.; Williams, T. N.; Kinyanjui, S.; Marsh, K.; Doolan,

D. L.; Engwerda, C.; Fowkes, F. J. I.; Grigg, M. J.; Mueller, I.; McCarthy, J. S.; Anstey, N. M.; Beeson, J. G. IgM in human immunity to plasmodium falciparum malaria. *Sci. Adv.* **2019**, *5*, No. eaax4489.
(16) Lee, H.-K.; Lee, B.-H.; Seok, S.-H.; Baek, M.-W.; Lee, H.-Y.; Kim, D.-J.; Na, Y.-R.; Noh, K.-J.; Park, S.-H.; Kumar, D. N.; Kariwa, H.; Nakauchi, M.; Heo, S.-J.; Park, J.-H. Production of specific antibodies against SARS-coronavirus nucleocapsid protein without cross reactivity with human coronaviruses 229E and OC43. *J. Vet. Sci.* **2010**, *11*, 165−167.
(17) Li, S.-F.; Tan, Y.-Z.; Tang, Y.-B.; Liu, L.-E.; Chen, W.-L. The Detect ion and Trace of SARS Coronavirus Antibodies. *J. Practical Med. Tech.* **2005**, *12*, 1380−1382.
(18) Turner, L. H.; Kinder, J. M.; Wilburn, A.; D'Mello, R. J.; Braunlin, M. R.; Jiang, T. T.; Pham, G.; Way, S. S. Preconceptual Zika virus asymptomatic infection protects against secondary prenatal infection. *PLoS Pathog.* **2017**, *13*, No. e1006684.
(19) Posthuma-Trumpie, G. A.; Korf, J.; van Amerongen, A. Lateral flow (immuno)assay: its strengths, weaknesses, opportunities and threats. A literature survey. *Anal. Bioanal. Chem.* **2009**, *393*, 569−582.
(20) Koczula, K. M.; Gallotta, A. Lateral flow assays. *Essays Biochem.* **2016**, *60*, 111−120.
(21) Zuo, J.-Y.; Jiao, Y.-J.; Zhu, J.; Ding, S.-N. Rapid Detection of Severe Fever with Thrombocytopenia Syndrome Virus via Colloidal Gold Immunochromatography Assay. *ACS Omega* **2018**, *3*, 15399−15406.
(22) Ge, X.; Zhang, W.; Lin, Y.; Du, D. Magnetic Fe_3O_4@TiO_2 nanoparticles-based test strip immunosensing device for rapid detection of phosphorylated butyrylcholinesterase. *Biosens. Bioelectron.* **2013**, *50*, 486−491.
(23) Huang, C.; Wei, Q.; Hu, Q.; Wen, T.; Xue, L.; Li, S.; Zeng, X.; Shi, F.; Jiao, Y.; Zhou, L. Rapid detection of severe fever with thrombocytopeniasyndrome virus (SFTSV) total antibodies by up-converting phosphor technology-based lateral-flow assay. *Luminescence* **2019**, *34*, 162−167.
(24) Lu, T.; Zhu, K.-D.; Huang, C.; Wen, T.; Jiao, Y.-J.; Zhu, J.; Zhang, Q.; Ding, S.-N. Rapid detection of Shiga Toxin type II by lateral flow immunochromatography test strips of colorimetry and fluorimetry. *Analyst* **2019**, *145*, 76−82.
(25) Song, C.; Liu, J.; Li, J.; Liu, Q. Dual FITC lateral flow immunoassay for sensitive detection of Escherichia coli O157:H7 in food samples. *Biosens. Bioelectron.* **2016**, *85*, 734−739.
(26) Carrio, A.; Sampedro, C.; Sanchez-Lopez, J.; Pimienta, M.; Campoy, P. Automated low-cost smartphone-based lateral flow saliva test reader for drugs-of-abuse detection. *Sensors* **2015**, *15*, 29569−29593.
(27) Gnoth, C.; Johnson, S. Strips of Hope: Accuracy of Home Pregnancy Tests and New Developments. *Geburtshilfe Frauenheilkd.* **2014**, *74*, 661−669.
(28) Le, T. T.; Chang, P.; Benton, D. J.; McCauley, J. W.; Iqbal, M.; Cass, A. E. G. Dual recognition element lateral flow assay toward multiplex strain specific influenza virus detection. *Anal. Chem.* **2017**, *89*, 6781−6786.
(29) Brangel, P.; Sobarzo, A.; Parolo, C.; Miller, B. S.; Howes, P. D.; Gelkop, S.; Lutwama, J. J.; Dye, J. M.; McKendry, R. A.; Lobel, L.; Stevens, M. M. A Serological Point-of-Care Test for the Detection of IgG Antibodies against Ebola Virus in Human Survivors. *ACS Nano* **2018**, *12*, 63−73.
(30) Aldewachi, H.; Chalati, T.; Woodroofe, M.; Bricklebank, N.; Sharrack, B.; Gardiner, P. Gold nanoparticle-based colorimetric biosensors. *Nanoscale* **2018**, *10*, 18−33.
(31) Jans, H.; Huo, Q. Gold nanoparticle-enabled biological and chemical detection and analysis. *Chem. Soc. Rev.* **2012**, *41*, 2849−2866.
(32) Cabuzu, D.; Cirja, A.; Puiu, R.; Grumezescu, A. Biomedical Applications of Gold Nanoparticles. *Curr. Top. Med. Chem.* **2015**, *15*, 1605−1613.
(33) Vilela, D.; González, M. C.; Escarpa, A. Sensing colorimetric approaches based on gold and silver nanoparticles aggregation: chemical creativity behind the assay. A review. *Anal. Chim. Acta* **2012**, *751*, 24−43.
(34) Yang, F.; Xiao, Y.; Chen, B.; Wang, L.; Liu, F.; Yao, H.; Wu, N.; Wu, H. Development of a colloidal gold-based immunochromatographic strip test using two monoclonal antibodies to detect H7N9 avian influenza virus. *Virus Genes* **2020**, DOI: 10.1007/s11262-020-01742-8.
(35) Ren, W.; Xu, Y.; Huang, Z.; Li, Y.; Tu, Z.; Zou, L.; He, Q.; Fu, J.; Liu, S.; Hammock, B. D. Single-chain variable fragment antibody-based immunochromatographic strip for rapid detection of fumonisin B1 in maize samples. *Food Chem.* **2020**, *319*, 126546.
(36) Liu, J.-Z.; Wang, J.-Y.; Li, Z.-H.; Meng, H.-M.; Zhang, L.; Wang, H.-Q.; Li, J.-J.; Qu, L.-B. A lateral flow assay for the determination of human tetanus antibody in whole blood by using gold nanoparticle labeled tetanus antigen. *Mikrochim. Acta* **2018**, *185*, 110.
(37) Huang, L.; Jin, J.; Wang, J.; Jiang, C.; Xu, M.; Wen, H.; Liao, T.; Hu, J. Homogeneous and high-density gold unit implanted optical labels for robust and sensitive point-of-care drug detection. *Nanoscale* **2019**, *11*, 16026−16035.
(38) Haiss, W.; Thanh, N. T. K.; Aveyard, J.; Fernig, D. G. Determination of size and concentration of gold nanoparticles from UV-vis spectra. *Anal. Chem.* **2007**, *79*, 4215−4221.
(39) Yokota, S. Preparation of Colloidal Gold Particles and Conjugation to Protein A, IgG, F(ab') 2, and Streptavidin. *Methods Mol. Biol.* **2010**, *657*, 109−119.
(40) Yuan, X.; Fabregat, D.; Yoshimoto, K.; Nagasaki, Y. Development of a high-performance immunolatex based on "soft landing" antibody immobilization mechanism. *Colloids Surf., B* **2012**, *99*, 45−52.
(41) Roth, J.; Bendayan, M.; Orci, L. Ultrastructural localization of intracellular antigens by the use of protein A-gold complex. *J. Histochem. Cytochem.* **1978**, *26*, 1074−1081.
(42) Frens, G. Controlled Nucleation for the Regulation of the Particle Size in Monodisperse Gold Suspensions. *Nature, Phys. Sci.* **1973**, *241*, 20−22.
(43) Oh, J.; Joung, H.-A.; Han, H. S.; Kim, J. K.; Kim, M.-G. A hook effect-free immunochromatographic assay (HEF-ICA) for measuring the C-reactive protein concentration in one drop of human serum. *Theranostics* **2018**, *8*, 3189−3197.
(44) To, K. K.-W.; Tsang, O. T.-K.; Leung, W.-S.; Tam, A. R.; Wu, T.-C.; Lung, D. C.; Yip, C. C.-Y.; Cai, J.-P.; Chan, J. M.-C.; Chik, T. S.-H.; Lau, D. P.-L.; Choi, C. Y.-C.; Chen, L.-L.; Chan, W.-M.; Chan, K.-H.; Ip, J. D.; Ng, A. C.-K.; Poon, R. W.-S.; Luo, C.-T.; Cheng, V. C.-C.; Chan, J. F.-W.; Hung, I. F.-N.; Chen, Z.; Chen, H.; Yuen, K.-Y. Temporal profiles of viral load in posterior oropharyngeal saliva samples and serum antibody responses during infection by SARS-CoV-2: an observational cohort study. *Lancet Infect. Dis.* **2020**, *20*, 565.
(45) Zhang, W.; Du, R.-H.; Li, B.; Zheng, X.-S.; Yang, X.-L.; Hu, B.; Wang, Y.-Y.; Xiao, G.-F.; Yan, B.; Shi, Z.-L.; Zhou, P. Molecular and serological investigation of 2019-nCoV infected patients: implication of multiple shedding routes. *Emerging Microbes Infect.* **2020**, *9*, 386−389.
(46) Grabar, K. C.; Freeman, R. G.; Hommer, M. B.; Natan, M. J. Preparation and characterization of Au colloid monolayers. *Anal. Chem.* **1995**, *67*, 735−743.
(47) Jiao, Y.; Zeng, X.; Guo, X.; Qi, X.; Zhang, X.; Shi, Z.; Zhou, M.; Bao, C.; Zhang, W.; Xu, Y.; Wang, H. Preparation and evaluation of recombinant severe fever with thrombocytopenia syndrome virus nucleocapsid protein for detection of total antibodies in human and animal sera by double-antigen sandwich enzyme-linked immunosorbent assay. *J. Clin. Microbiol.* **2012**, *50*, 372−377.

https://dx.doi.org/10.1021/acsomega.0c01554
ACS Omega 2020, 5, 12550−12556